NON-MONOTONE SELECTION STRENGTH AND THE EMERGENCE OF ANTIBIOTIC RESISTANCE

Rafael C. Reding[1†], & Robert E. Beardmore[1]
[1]*College of Life and Environmental Sciences, University of Exeter*
[†] E-mail: rcr202@exeter.ac.uk, @rc_reding

EPSRC Engineering and Physical Sciences Research Council
UNIVERSITY OF EXETER

WHAT IS THE ROLE of selection in the emergence of antibiotic resistance? This phenomenon is thought to arise within specific concentrations of antibiotic known as the *mutant selection window* (MSW),[1] where mutants are selected at specific, fixed concentrations of antibiotic. However, it was later shown that selection of resistance can occur outside this window.[2] This has been explained based on ecological interactions as the main driver of the emergence of resistance. This process, known as *competitive release*,[3] suggests that the clearance of susceptible microbes by antibiotics let resistance flourish with plenty of resources, taking place within a specific concentration of antibiotic. This idea assumes pre-existent microbial diversity and is driven by elementary population genetics, for which the strength of selection is directly proportional to the strength of the selection pressure (antibiotic concentration).[4,5] This principle is demonstrated in the short-term by the so-called susceptibility tests,[6] whereby the clearance of microbes is proportional to the dose of the antibiotic used, but does this proportionality hold at all times?

I. METHOD

We addressed this question using a combination of mathematical modelling and evolutionary experiments based on different modifications of the wild type strain of *Escherichia coli* K-12, focusing on the multidrug efflux pump system AcrAB-TolC, and compared the results for each of them. For this latter purpose, we used batch cultures grown in 96-wells microplates and certified the linear relationship between cell density and optical density measured at λ = 600$_{nm}$ (OD_{600}).

Mathematical model

The concept and assumptions that we based our mathematical model on are summarised as follows:

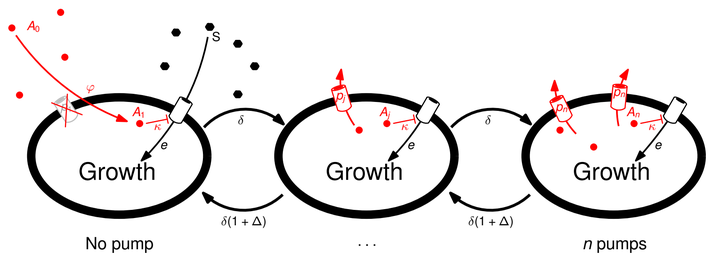

FIGURE1. Representation of the mathematical model that we used to address our question. A carbon source S and an initial dose of antibiotic A_0 are supplied in the environment. Each cell contains an enzyme able to take S from the environment, and process it with an efficiency e in order to grow . At the same time, A diffuses into the cell at a rate φ, and binds to the enzyme with an affinity κ interrupting the cell growth. The cells may remove A with a generic mechanism of resistance such as an efflux pump ρ,[7,8] contained in different numbers depending on the genotype, reducing the effect of A on cell growth. Cells can 'mutate' and see their efflux pumps increased or reduced as a function of δ. We assume that the efflux pump may incur in a metabolic cost, Δ.

Quantifying antibiotic sensitivity

To quantify the sensitivity of *E. coli*, we defined cell growth in terms of OD_{600} as a function of antibiotic concentration ('dose-response' profile) and calculated the concentration of antibiotic inhibiting 99% of growth compared to an antibiotic-free condition. The strains used are AG100 (wild type), AG100-A ($\triangle$*acrAB*), TB108 (*acrB-sfGFP*) and eTB108 (evolved TB108). We measured cell growth both in terms of OD_{600}, and normalised fluorescence (nGFP). We used the ratio nGFP per OD_{600} as a proxy for the number of copies of the *acr* operon including *acrB*. The antibiotic used is the macrolide erythromycin.

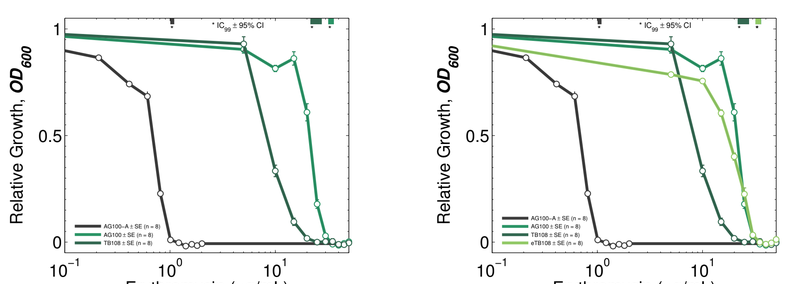

FIGURE2. Dose-response profiles for the different strains of *E. coli* measured after 24h. The plot in the left reflects the intermediate sensitivity of the strain TB108 due to the interfering sfGFP. The evolved strain (eTB108) shows an identical sensitivity to erythromycin after a week of growth with 10μg/mL of erythromycin. OD_{600} is represented in the y-axis, whilst the concentration of erythromycin is represented in logarithmic scale in the x-axis. The IC_{99}± 95% confidence interval is shown for each strain on top of the x-axis.

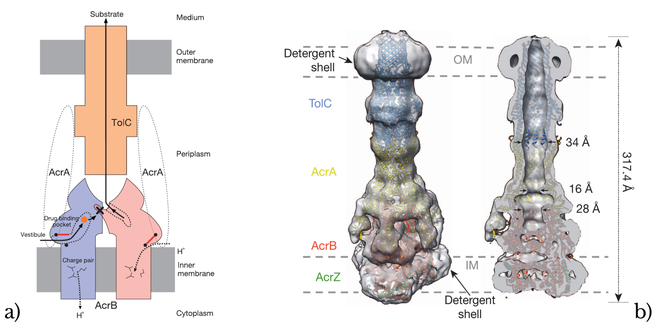

FIGURE3. Proposed transport mechanism (a), and structure of the multidrug efflux pump AcrAB-TolC (b) from REFERENCES 9 (a) and 10 (b). The pump rests on a structure formed by AcrB and AcrZ in the inner membrane, opened to the cytoplasm. In the outer membrane lies TolC forming a pore opened to the environment. AcrA connects both in the periplasm, and forms a vestibule in the periplasm with AcrB. The drug binding pocket is hidden in the vestible. The drug is captured and ejected to the environment powered by protons (H^+) from the periplasm. Note that further studies of this pump allowed to establish the cytoplasmic section of AcrB as a completely different component, AcrZ also produced by the *acr* operon.

Quantifying evolution

We computed cell growth (G) by fitting the following models using the functions `fitlm` and `fitnlm` as implemented in MATLAB 2014A

$$G(t) = G_0 + t \cdot r, \tag{1a}$$
$$G(t) = G_0 + C^{t \cdot r}, \tag{1b}$$
$$G(t) = G_0 + \frac{K}{1 + C \cdot e^{-t \cdot r}} \tag{1c}$$

G_0 being the cell growth at t=0h, K the carrying capacity, r the per capita growth rate, and $C \gg 1$ a correction factor G_0-dependant. We calculated the best fit as the model with the lowest corrected Akaike information criterion (AICc). Based on fitted data (F), we later calculated the area under the curve (AUC) to estimate the growth rate as

$$AUC := \int_0^{24h} F(t) \cdot dt, \tag{2a}$$
$$AUC_{24h} := \int_{24h-\Delta}^{24h} F(t) \cdot dt, \tag{2b}$$
$$r(h^{-1}) := AUC_{24h} \cdot AUC^{-1} \cdot \Delta^{-1} \tag{2c}$$

Δ being the time interval at which the cultures were read (1/3h). To quantify evolution, we used the so-called 'rate of adaptation'[11] (α). The rate of adaptation is defined as the relationship between Δr and the adaptive time (t_a), Δr being the difference between the growth rates at the beginning and at the end of the experiment (see FIGURE 4).

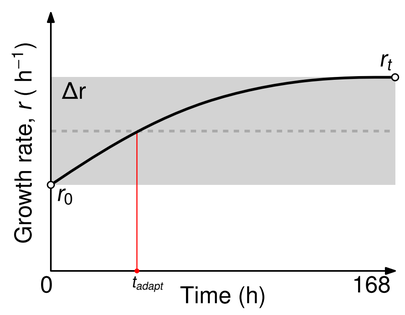

FIGURE4. Rationale to measure the rate of adaptation (α). The growth rate, r, changes through time as the culture adapts to the environmental conditions. We define the adaptive time (t_a) as the time at which the condition $r = r_0 + \Delta r/2$ is satisfied. The rate of adaptation is thus defined as $\alpha := \frac{\Delta r/2}{t_a}$. We use the notation α_{AUC} to denote that the growth rate that we used is based on AUC.

II. RESULTS

Model prediction

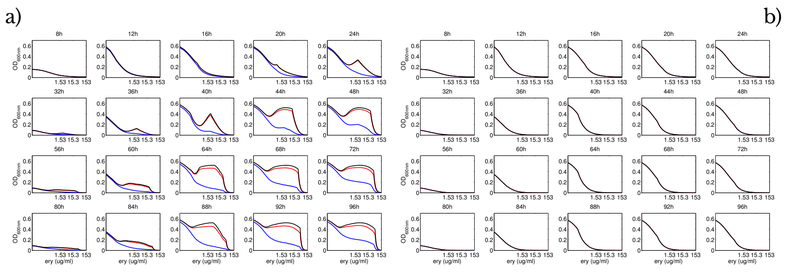

FIGURE5. Prediction from our mathematical model. The concentration of antibiotic is represented in the x-axis, whereas the growth in terms of OD_{600} is represented on the y-axis. The black line shows the total population, conformed by bacteria without the efflux pump (blue), and with one copy of the efflux pump (red). This model states that the initial antimicrobial dose-response profile is monotone. Nevertheless, different genotypes with increasing number of pumps appear and are selected by increasing doses of antibiotic turning the monotone dose-response profile into a non-monotone profile. The plateau in the blue subpopulation is produced by the loss of efflux pumps from other genotypes. Starting with an 'inoculum' of cells with no pumps, in a) we represent the prediction when $\delta > 0$ whereas in b) is the prediction when $\delta = 0$

Experimental results

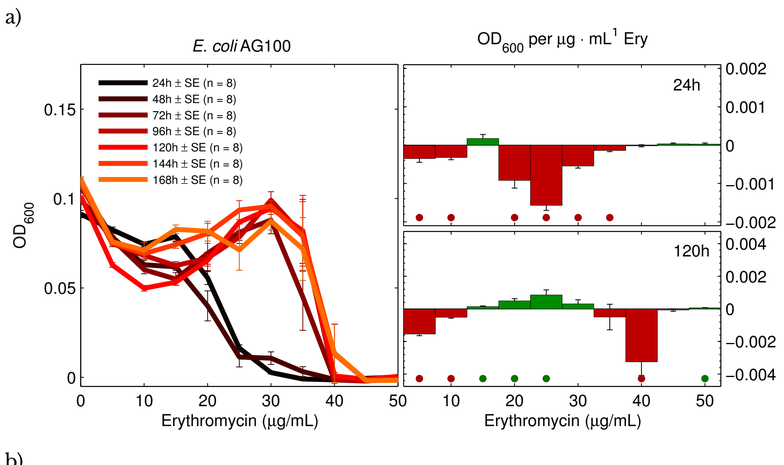

FIGURE6. Erythromycin dose-response profiles for the strains of *E. coli* AG100 (a) and AG100-A (b) measured every 24h (± standard error of the mean, n=8). The readings for OD_{600} are represented in the y-axis, and the concentration of erythromycin is represented in the x-axis. For the subplots, the y-axis represent the slope of the dose-response profiles. In this latter case, the slopes were measured in intervals of 5 (a) and 0.2 (b) μg/mL of erythromycin, and using a tailored, unpaired t-test we looked for significantly positive (green dots) or negative (red dots) slopes with $\alpha = 0.01$. The top subplot shows the result of this analysis at t=24h, whereas the bottom subplot shows the result at t=120h. Having (a) or not (b) the multidrug efflux pump AcrAB-TolC drives the ability of *E. coli* to respond non-monotonically to erythromycin, as predicted by our model.

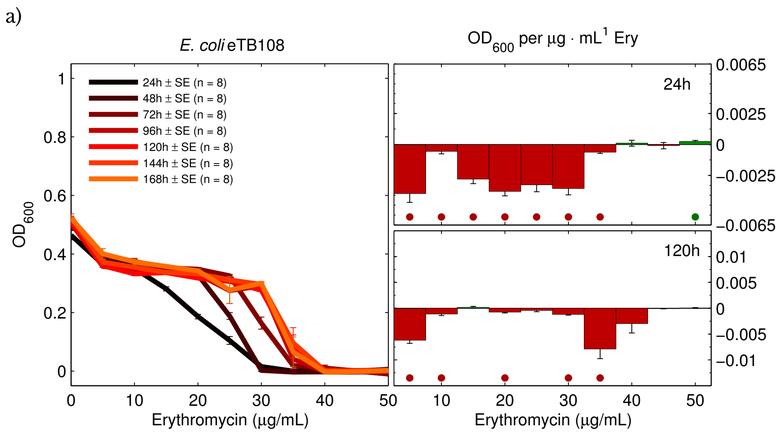

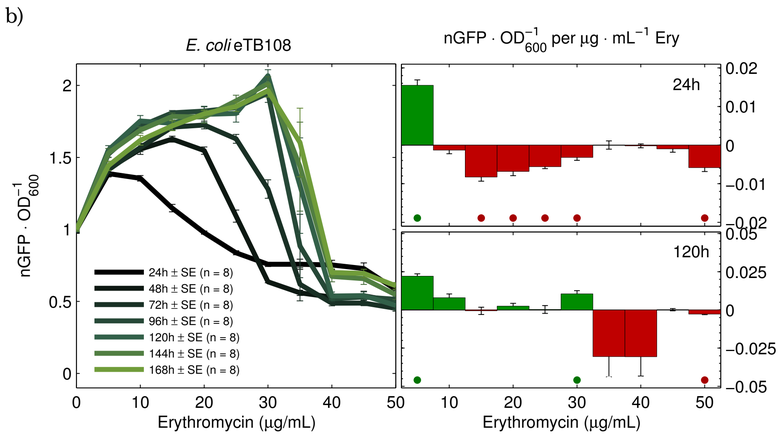

FIGURE7. Erythromycin dose-response profiles for the strains of *E. coli* eTB108 measured every 24h (± standard error of the mean, n=8). The readings for OD_{600} (a) or relative normalised GFP per OD_{600} (b) are represented in the y-axis, and the concentration of erythromycin is represented in the x-axis. For the subplots, the y-axis represent the slope of the dose-response profiles. In this latter case, the slopes were measured in intervals of 5μg/mL of erythromycin, and using a tailored, unpaired t-test we looked for significantly positive (green dots) or negative (red dots) slopes with $\alpha = 0.01$. The top plot shows the result of this analysis at t=24h, whereas the bottom plot shows the result at t=120h. In this case, the dose-response profile remains monotone at 24h intervals in terms of OD_{600}, although with a significant increase in the slope through time. This increase overlaps with an non-monotone increase in the relative normalised GFP per OD_{600}, the fastes sweep occurring with 30μg/mL of erythromycin.

Evolutionary 'coldspots' & 'hotspots'

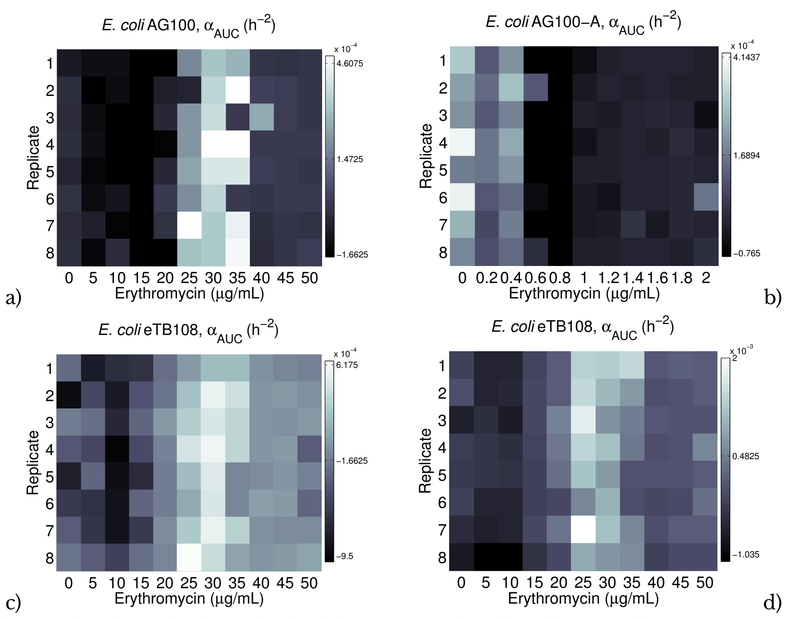

FIGURE8. Selection landscape for the different strains of *E. coli* as a function of the concentration of erythromycin. The plots show the rate of adaptation per replicate based on AUC (α_{AUC}). Black colour represents the lowest rate of adaptation, whereas white colour represents the highest. Note the existence of a 'window' where the rate of adaptation the highest, and another 'window' where the adaptation is the lowest. Moreover, the second 'window' sits below the antibiotic-free level, suggesting the existence of concentrations of antibiotic were adaptation has been slower in the presence of erythromycin than in its absence.

III. DISCUSSION

The existence of evolutionary 'coldspots' and 'hotspots' challenges the principle formerly introduced whereby selection is directly proportional to the strength of selective pressure (here antibiotics). This non-linearity in the selection landscape is a signature quantifiable when the sensitivity to erythromycin becomes non-monotone through time, caused in our system by the varying number of the multidrug efflux pump AcrAB-TolC. The boundaries of the 'hotspots' do not match those of the MSW,[1] but the non-linear nature of selection may help to a better of the emergence through time of resistance to antibiotics.

REFERENCES

1. Baquero, F. & Negri, M.-C. Challenges: Selective compartments for resistant microorganisms in antibiotic gradients. *Bioessays* **19**, 731–736 (1997).
2. Gullberg, E. *etal.* Selection of resistant bacteria at very low antibiotic concentrations. *PLoS Pathog.* **7**, e1002158 (2011).
3. Day, T., Huijben, S. & Read, A.F. Is selection relevant in the evolutionary emergence of drug resistance? *Trends in Microbiology* **23**, 126–133 (2015).
4. Read, A.F., Day, T. & Huijben, S. The evolution of drug resistance and the curious orthodoxy of aggressive chemotherapy. *Proc. Natl. Acad. Sci. U.S.A.* **108**, 10871–10877 (2011).
5. Ankomah, P. & Levin, B.R. Exploring the collaboration between antibiotics and the immune response in the treatment of acute, self-limiting infections. *Proc. Natl. Acad. Sci. U.S.A.* **111**, 8331–8338 (2014).
6. Clinical and Laboratory Standards Institute. *Performance Standards for Antimicrobial Susceptibility Testing; Twenty–Second Informational Supplement M100–S22* (2012).
7. Van Bambeke, F., Balzi, E. & Tulkens, P.M. Antibiotic efflux pumps. *Biochemical pharmacology* **60**, 457–470 (2000).
8. Webber, M. & Piddock, L. The importance of efflux pumps in bacterial antibiotic resistance. *J. Antimicrob. Chemother.* **51**, 9–11 (2003).
9. Murakami, S., Nakashima, R., Yamashita, E., Matsumoto, T. & Yamaguchi, A. Crystal structures of a multidrug transporter reveal a functionally rotating mechanism. *Nature* **443**, 173–179 (2006).
10. Du, D. *etal.* Structure of the AcrAB-TolC multidrug efflux pump. *Nature* **509**, 512–515 (2014).
11. Hegreness, M., Shoresh, N., Damian, D., Hartl, D. & Kishony, R. Accelerated evolution of resistance in multidrug environments. *Proc. Natl. Acad. Sci. U.S.A.* **105**, 13977–13981 (2008).